Finding the windows of regular motion within the chaos of ordinary differential equations

Alice D. Churukian* and Dale R. Snider
Physics Department, University of Wisconsin–Milwaukee, Milwaukee, Wisconsin 53201
(Received 18 July 1995; revised manuscript received 6 September 1995)

A method is presented to find the windows of regular motion, which are normally buried in the chaos, of ordinary differential equations. It relies on using the Hénon map to approximate the Poincaré map of the differential equations. Here, it is demonstrated for the physical system of a vertically driven, damped pendulum.

PACS number(s): 05.45.+b, 03.20.+i, 02.90.+p

INTRODUCTION

We use the Hénon map to approximate the Poincaré return map of a dynamical system of three ordinary differential equations (ODE's). The Hénon map [1], a two-dimensional map with two parameters a and b, is

$$x_{n+1}=1-ax_n^2+y_n\ ,\quad y_{n+1}=bx_n\ . \tag{1}$$

It is general enough to approximate any two-dimensional map that has a fixed point and a fixed contraction per iteration, through the quadratic terms in an expansion about the fixed point. Gallas [2] has recently found the positions of the windows of regular motion of the Hénon map as a function of its two parameters. This information could be used to find the corresponding windows of the dynamical system if one knew how to determine the parameters of the approximating Hénon map from the parameters of the dynamical system described by the ODE's. One of these parameters can usually be determined by equating the rates of contraction of a comoving volume in the two systems. Then we are left with finding the value of the other parameter, which produces the desired regular behavior. The value of this parameter can be determined by studying the behavior of the Hénon map near the desired window and then seeking this behavior in the dynamical system by a search strategy of bracketing and successive halving.

THE VERTICALLY DRIVEN, DAMPED PENDULUM

As an example of this method, we consider the case of the vertically driven, dampled pendulum. We choose this system because its response is richer than the simple pendulum. Taking the force frequency "at resonance," the differential equation is

$$\frac{d^2\theta}{dt^2}=-\sin\theta-\beta\frac{d\theta}{dt}+A\cos(2t)\sin\theta\ , \tag{2}$$

where A is the forcing amplitude and β is the damping factor. It is the extra factor of $\sin\theta$ in the forcing term that makes this different from the simple pendulum [3]. For instance, $\theta(t)=0$ is a solution to this equation for any forcing amplitude. For this vertically forced pendulum, the resonance frequency (for small amplitude) is twice the natural frequency of the unforced pendulum, hence the factor of 2 in the above equation. If we let $\omega=d\theta/dt$ and ϕ be the phase of the forcing term, then we can rewrite this as three autonomous first-order differential equations

$$\dot\theta=\omega\ ,$$
$$\dot\omega=-\sin\theta-\beta\omega+A\cos\phi\sin\theta\ , \tag{3}$$
$$\dot\phi=2\ .$$

In this three-dimensional space the rate of relative contraction of a comoving volume is β. We take the Poincaré section at fixed ϕ and the Poincaré map to be the second return map, giving the values of ω and θ at $\phi=\phi_0+4\pi$ as a function of those values at $\phi=\phi_0$. Then the contraction per iteration of an area, induced by the Poincaré map, is $e^{-2\pi\beta}$.

BEHAVIOR OF THE VERTICALLY DRIVEN, DAMPED PENDULUM [3]

We have examined the behavior of the vertically driven, damped pendulum by fourth-order Runge-Kutta numerical integration with 60 steps per 2π forcing cycle. One way to display this behavior of the pendulum on the computer is to make a plot of the motion in the θ-ω plane, ignoring ϕ. We use a distorted θ-ω plane to keep θ continuous even for over-the-top (i.e., rotational) motion. We do this by using quasipolar coordinates where θ is plotted as an angle, while ω is plotted radially starting at a zero circle, with the positive direction being toward the center of the circle; see Fig. 1. Of course, one must watch the scale for ω so that it never becomes so large as to make the radius vector negative. This plot has the virtue that for small oscillations it looks similar to a Cartesian plot, while for over-the-top motion it produces a continuous path.

The behavior of the vertically driven pendulum is very rich. When we fix the damping coefficient, at $\beta=0.5$ for example, and increase the driving amplitude A from zero, we find the following behaviors, which are shown in Fig. 2:

(a) fixed point at rest,

(b) symmetric one-cycle (the standard resonance motion),

*Present address: Physics Department, Thaddeus Stevens State School of Technology, Lancaster, PA 17602.

1063-651X/96/53(1)/74(6)/$06.00

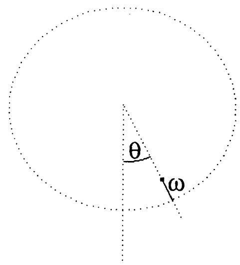

FIG. 1. Distorted θ-ω plane used to plot the projection (ϕ is ignored) of the phase-space motion of the vertically driven, damped pendulum. Here θ is plotted as an angle, while $\omega = d\theta/dt$ is plotted radially from a zero circle, inward being positive.

(c) spontaneous symmetry breaking to an *asymmetric* one-cycle,

(d) bifurcation to an asymmetric two-cycle,

(e) repeated bifurcations of the period-doubling route to chaos,

(f) asymmetric chaotic motion,

(g) crisis to symmetric chaotic motion, and

(h) another crisis to over-the-top chaotic motion.

It is in the region of asymmetric chaotic motion, behavior (f), where we wish to find the windows of regular motion. There must be an unstable asymmetric one-cycle buried in the asymmetric strange attractor. It is the continuation of the stable asymmetric one-cycle found at lower values of A in region (c) above. This fixed point in the Poincaré section, not the one at $\theta=0=\omega$, is the center of the region which the Hénon map is approximating.

COMPARISON WITH THE HÉNON MAP

Note that the Hénon map collapses into the one-dimensional logistic map if $b=0$. The variable y is lost, while x takes on the role of the single variable of the logistic map. Metropolis, Stein, and Stein [4] have studied and characterized by a unique code each window of regular motion of the logistic map.

The contraction of a comoving area in the Hénon map is $|b|$. Thus, if the Hénon map is going to approximate the Poincaré map of the pendulum's dynamics we must have $|b|=e^{-2\pi\beta}$. Note that this implies that *larger* damping brings the pendulum's dynamics closer to the logistic map, with its well known results. We are still free to choose the value of ϕ_0 where we take the Poincaré section. With a judicious choice of ϕ_0, the mapping of the Hénon map onto the Poincaré map might allow one of the two variables θ or ω, and not a linear combination of the two, to essentially correspond to x in the Hénon map. We found that such a choice allowed θ to be the desired quantity. (This occurs at the ϕ_0 where the strange attractor in the θ-ω plane lies mainly in the θ direction.) By comparing the position of the extra arm in the plot of θ_{n+1} vs θ_n to the corresponding plots of x_{n+1} vs x_n, we found that *negative b* is necessary for the Hénon map to approximate the Poincaré map; see Figs. 3 and 4. Thus we have

$$b=-e^{-2\pi\beta} . \tag{4}$$

This is one of two needed relations to determine which Hénon map approximates a particular vertically driven, damped pendulum. Unfortunately, we know of no general principle that can tell us the other relationship $a=a(A,\beta)$, so we must resort to a searching algorithm. Any window of the Hénon map that can be directly continued to $b=0$ (normal window) can be identified with the Metropolis-Stein-Stein (MSS) code of the logistic map. Even for $b<0$ the code still describes the dynamics of the periodic behavior. However, there exists windows that do not continue to $b=0$; instead, they are the "shrimp" windows discovered and named by Gallas. They cannot be assigned a unique binary code since they have two points at or near the peak of x_{n+1} vs x_n, one on the parabola and the other on the extra arm.

In Fig. 5 we have made an enlargement of Gallas's diagram for the range of parameters that apply to the pendulum, i.e., negative b. Here black is chaotic motion and white is regular, or, at the high-a limit, unbounded. The trajectories of nine normal windows appear. Using their MSS code at $b=0$, they are the ten-cycle RLR^3LRLR, the six-cycle RLR^3, the eight-cycle RLR^5, the seven-cycle RLR^4, the five-cycle RLR^2, another seven-cycle RLR^2LR, the three-cycle RL, another five-cycle RL^2R, and the four-cycle RL^2. One of the shrimp windows, an eight-cycle, may be seen at $a=1.8$ and $b=-0.024$. Traces of other narrower windows are also evident. Two of the windows (the three- and four-cycles) slope down to the left, while the other seven slope down to the right. The first two also terminate before $b=-0.05$, while the other seven do not terminate in this range. (The five-cycle RL^2R does, however, hit the crisis.) The difference between these two behaviors is related to the extra arm on the plot of x_{n+1} vs x_n.

The extra arm is the image of points to the left of the peak while the "parabola" is the image of points to the right of the peak. Thus the last letter of the MSS code determines whether the peak point will be on the parabola or on the extra arm. If the last letter is R then the peak point will be on the parabola and the trajectory of the window will slope to higher a as b decreases. If it is L then the peak point will be on the extra arm and the slope will be in the other direction. (If the strange attractor were "fatter" it is possible that we would see more layers and would then have to specify the last two letters of the code to specify the layer of the peak point.) The peak point being on the extra arm also seems to cause termination of the window. In this region of the parameter space there are two possible asymptotic behaviors, chaotic or periodic, depending on the initial conditions. These three- and four-cycle windows terminate by the basin of attraction of the periodic behavior shrinking until it vanishes.

Thus, by examining Gallas's diagrams, we learn that most of the windows at $b=-0.05$ continue back to $b=0$, where they are the standard windows of the logistic map. The two notable exceptions are the three-cycle window of the logistic map, which "closes" before it reaches the interesting b values, and a new set of eight-cycle win-

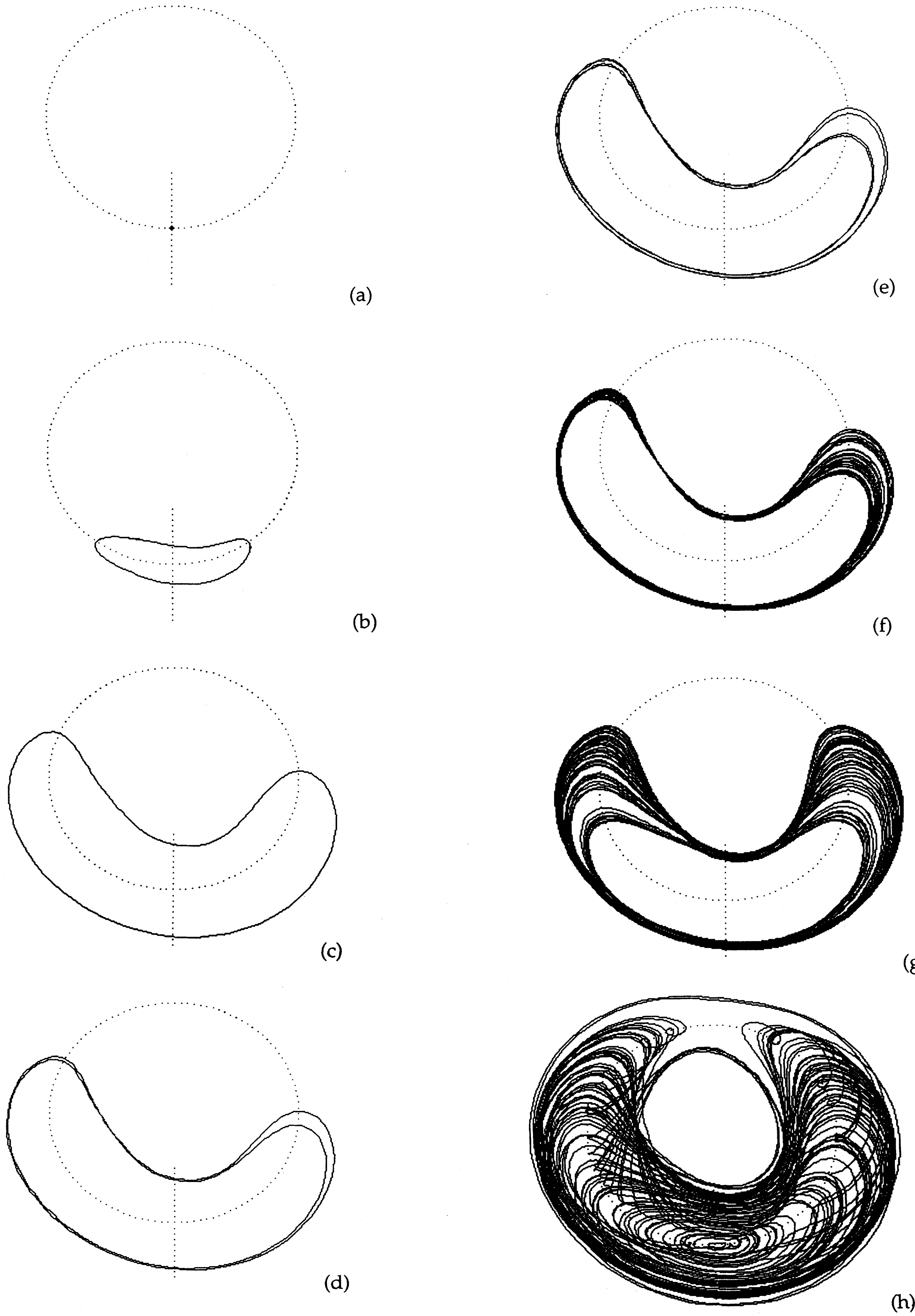

FIG. 2. Various attractors of the vertically forced pendulum. The driving amplitude A is being increased while the damping is fixed: (a) the motion dies out (in spite of being driven), (b) a symmetric cycle, (c) an asymmetric cycle, (d) an asymmetric two-cycle, (e) an asymmetric four-cycle, (f) asymmetric chaotic motion, (g) symmetric chaos, and (h) over-the-top chaotic motion.

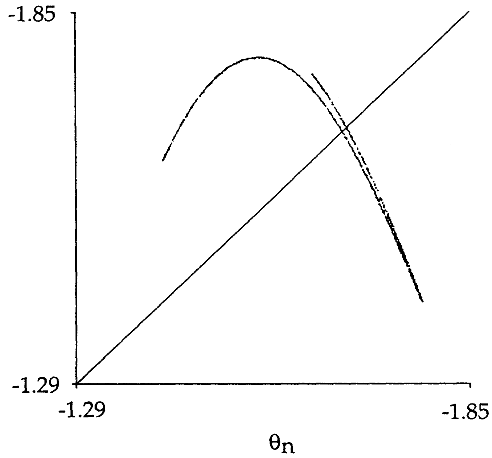

FIG. 3. Plot of θ_{n+1} vs θ_n from the Poincaré map of the vertically driven, damped pendulum in the asymmetric chaos regime. This is from the ϕ_0 where the strange attractor lies mainly in the θ direction, not the ω direction.

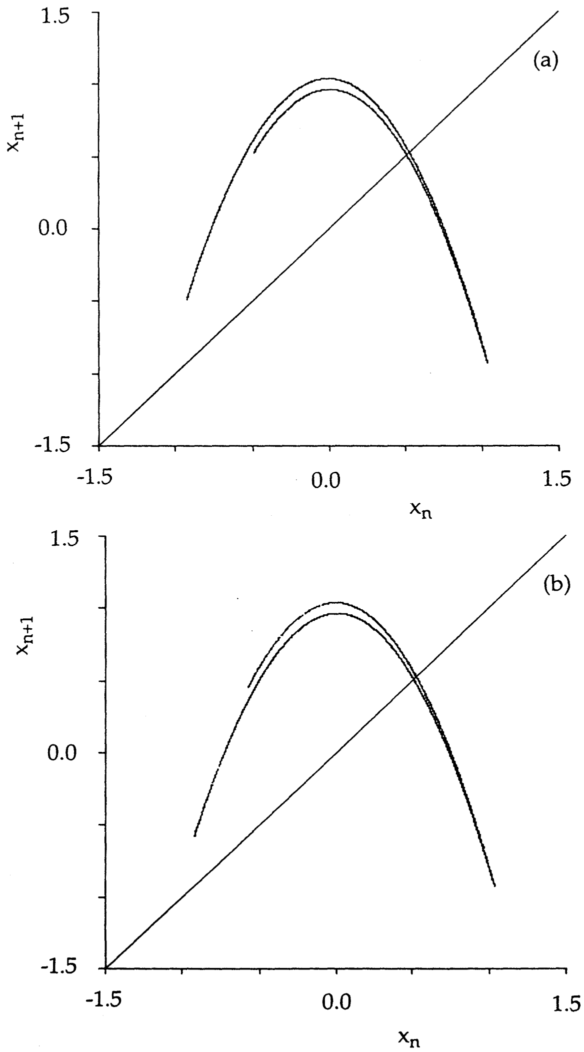

FIG. 4. Plots of x_{n+1} vs x_n from the Hénon map where it has chaotic motion, for two signs of b: (a) $b>0$ and (b) $b<0$. Note the position of the "extra arm" relative to the larger "parabola." The extra arm shrinks to nothing as $b \rightarrow 0$.

dows that come from an eight-cycle "shrimp," a region of regular structure that Gallas found.

THE SEARCH PROCEDURE

Let us assume that we want to find the value of A where a particular n-cycle window occurs for a given value of the damping factor β. We know to look in the Hénon map at $b=-e^{-2\pi\beta}$. From Gallas's work we can find the a value of the desired window. Then we need to relate this to the A value of the pendulum. The correspondence between the pendulum and the Hénon map is such that increasing a at fixed b implies increasing A at fixed β.

This also corresponds to increasing R in the logistic map. If the desired window is not one of the shrimp windows it can be continued to $b=0$, where it is a window of the logistic map and has a MSS [4] binary code. At the R value that makes the n-cycle superstable R_n, n iterations of the peak point $x_0=\frac{1}{2}$ returns to $x_n=\frac{1}{2}$. For R values near R_n, where $R=R_n+\delta R$, the nth iteration, starting at the same x_0, will yield $x_n=\frac{1}{2}+\delta x$. The sign of the derivative $\delta x/\delta R$ can be determined by the MSS code for

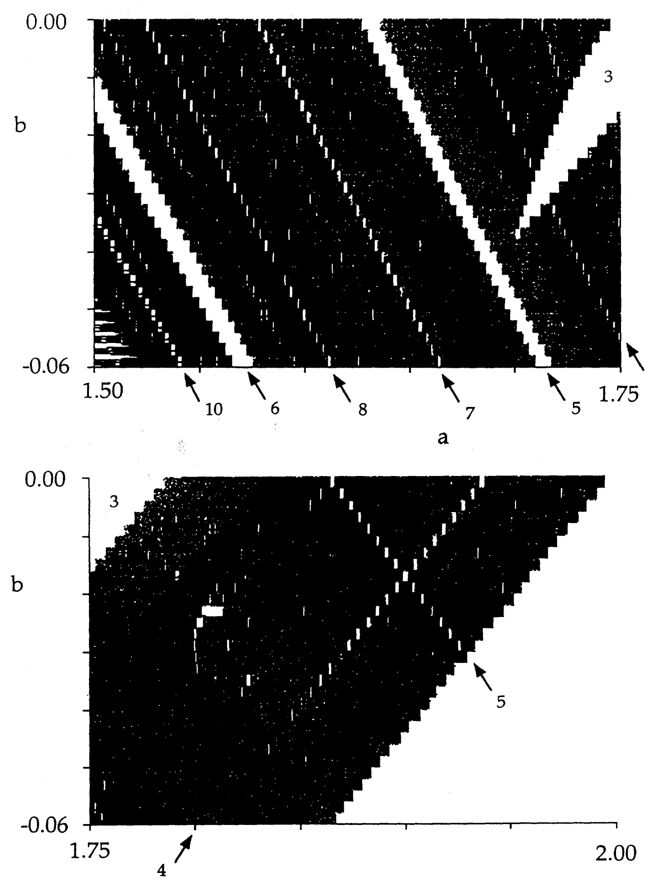

FIG. 5. Asymptotic motion (regular, chaotic, or unbounded) of the Hénon map as a function of a and b. Unfortunately, the diagram had to be cut into two to show enough detail. Black is chaotic, the white at large a is unbounded motion. The white lines are the windows of periodic motion; their periods are shown. The text further identifies them by their MSS codes.

TABLE I. Position of certain windows of periodic motion for the vertically driven, damped pendulum and for the corresponding Hénon map. The first column gives the order and the MSS binary code [4] of the window. The parameters A and β are for the pendulum, while a and b are the corresponding parameters of the Hénon map. For the pendulum, these parameters were obtained using fourth-order Runge-Kutta numerical integration with 60 steps per 2π forcing cycle.

Window	A	β	a	b
4 *RLR*	2.155 12	0.598	1.34	−0.023 3
6 *RLRRR*	1.901 38	0.48	1.55	−0.049
6 *RLRRR*	1.943 51	0.5	1.541	−0.043 2
6 *RLRRR*	2.154 45	0.595	1.5149	−0.023 8
7 *RLRRRR*	1.904 42	0.48	1.6472	−0.049
5 *RLRR*	1.746 23	0.4	1.742	−0.081
5 *RLRR*	1.864 65	0.46	1.7045	−0.055 6
5 *RLRR*	1.906 03	0.48	1.6955	−0.049
5 *RLRR*	1.948 25	0.5	1.687	−0.043 2
7 *RLRRLR*	1.907 42	0.48	1.7392	−0.049
7, 3	2.154 50	0.592	1.705	−0.024 24
3 *RL*	2.244 5	0.63	1.721	−0.019 1
3 *RL*	2.3410	0.67	1.728	−0.014 85
4 *RLL*	2.159 69	0.591	1.8855	−0.024 4
8 shrimp	2.162 345	0.5936	1.806	−0.024

the window. If the number of R's in the code is even then the derivative is positive, if odd then negative. This derivative may also be experimentally determined in the chaos outside the window of regular motion. It can be determined for either the Hénon map or the Poincaré map of the pendulum's dynamics. In these cases starting at the peak of the x_{n+1} vs x_n plot, or the θ_{n+1} vs θ_n plot, is the equivalent starting point. In the case of the Poincaré map, one cannot "start" at the peak since one does not know what ω to use. Instead, one must watch the θ_{n+1} vs θ_n plot as one integrates the differential equations and notes a point sufficiently near the peak. Then, after n more cycles, one can learn the sign of $\delta\theta$. This,

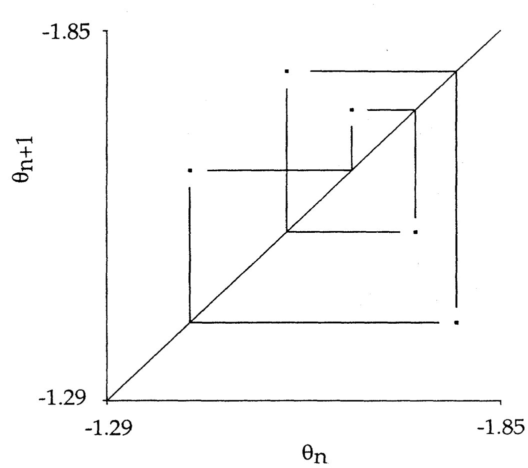

FIG. 6. Plot of θ_{n+1} vs θ_n for one of the windows of the vertically driven pendulum found at $A=1.906\,03$ and $\beta=0.48$. Lines have been added to help follow this five-cycle *RLRR*.

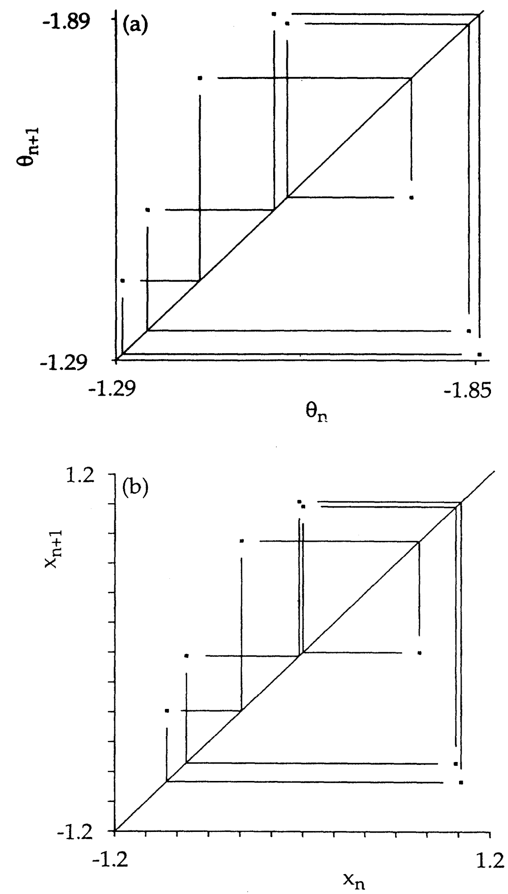

FIG. 7. Plots of the eight-cycle shrimp window: (a) θ_{n+1} vs θ_n from the vertically driven pendulum with $A=2.162\,345$ and $\beta=0.5936$ and (b) x_{n+1} vs x_n from the Hénon map with $a=1.806$ and $b=-0.024$. Note the similarity in the two plots.

along with the previously determined sign of the derivative, allows one to determine if this A value is above or below the desired A_n. Always staying in the region of asymmetric chaotic motion, region (f) above, one can bracket the desired A_n by repeating this process while varying A until the sign of $\delta\theta$ changes. Once one has bracketed the desired A_n, successive halving of the A interval allows the determination of A_n to any desired accuracy. By this procedure we have been able to find most of the windows with $n \leq 7$. See Table I. Figure 6 shows the θ_{n+1} vs θ_n plot of a five-cycle window.

Each of Gallas's shrimp windows lies at a particular a and b. Thus, to find a shrimp window in the pendulum's dynamics, one must be at the corresponding value of β. Then one again studies the behavior in the Hénon map at a values above and below the window's a value. From this, one is able to identify these behaviors in the Poincaré map, bracket the window, and finally home in on it. Figure 7 shows the plots of x_{n+1} vs x_n and of θ_{n+1} vs θ_n for the eight-cycle shrimp window.

Gallas's diagram shows where certain windows cross. We investigated this and found a set of parameters for the pendulum where, depending on the initial conditions, one ends on either the seven-cycle or the three-cycle. (See Table I.) To obtain the three-cycle one must be decreasing A to the given value. For the three-cycle at other parameter values and the four-cycle RLL, one either obtains chaos or the indicated n-cycle, depending on initial conditions. The basin of attraction for regular behavior shrinks as one decreases the value of b, starting from 0. These windows finally close when their basins of attraction shrink to nothing.

SUMMARY

As our table indicates, we have been able to find many of the windows of regular motion in the motion of the vertically driven, damped pendulum. Just as important, we have also learned where and why certain expected windows, such as the three-cycle, are absent. The discovery of these windows allows a "control of chaos" by choosing the parameters that keep the asymptotic behavior within a window of regular behavior.

This method of finding the windows of regular motion could be repeated for many dynamical systems described by three ODE's. However, it is not completely general. It probably does not work for a system with an internal symmetry. That is why we did not try it in region (g), where the asymptotic motion is symmetric chaos. In fact, an interesting question that remains is, "What is the nature of the Poincaré map when this symmetry exists?"

[1] M. Hénon, Commun. Math. Phys. **50**, 69 (1976).
[2] J. A. C. Gallas, Phys. Rev. Lett. **70**, 2714 (1993).
[3] As far as we know, the chaos of the vertically driven pendulum has not been discussed in the literature.
[4] N. Metropolis, M. L. Stein, and P. R. Stein, J. Comb. Theory **15**, 25 (1973).